6

3-APTMS mediated rapid synthesis of Ag@AuPd trimetallic nanoparticles

6.1. INTRODUCTION

Noble metal NPs have attracted a great deal of attention in many scientific and technological fields, due to the unusual properties they possess that leads to potential applications (Link and El-Sayed, 1999; Evanoff et al., 2004; Naoi et al., 2004; Frederix et al., 2003; Haruta, 1999; Bastakoti et al., 2015; Wang et al., 2011; Wang and Yamauchi, 2009). Multimetallic NPs composed of two or more metal elements with various nanostructures obtained via different synthesis approaches have presented improved physical and chemical properties compared to their monometallic components in many fields, especially in catalysis (El-Sayed, 2004; Wang et al., 2005).For this purpose, mono-, bi-, tri- and multi-metallic nanoparticles in solutions have been prepared with appreciable stability using a variety of capping agents such as surfactant micelles, functional polymers, dendrimers and so forth (Gong et al., 2010; Ikegami and Hamamoto, 2009). A central problem of the stabilizing agents is their strong interactions with metal NPs, which may alter the catalytic properties of the NPs. Moreover, leaching of heavy metals or even dissolution may be another problem for the recovery and reuse of metal NPs (Astruc et al., 2005; Akiyama and Kobayashi, 2009). Metal nanocatalysts have found a wide range of applications including CO oxidation

(Lang et al., 2004), carbon nanotube nucleation (Ago et al., 2003), alcohol dehydrogenation (Mitsudome et al., 2008) and formic acid electrooxidation (Waszczuk et al., 2002).

One of the potential applications of these nanoparticles is the reduction of p-Nitrophenol (PNP) (Pradhan et al., 2001).PNP, as with other nitrophenols and derivatives, is a common by-product of pesticides, herbicides and synthetic dyes (Vincent et al., 2003). Coinage metals, in particular, have been demonstrated to be excellent catalysts for PNP reduction on the nanoscale. Bimetallic coinage metal nanoparticles have been demonstrated to catalyze PNP reduction with rates that strongly differ from a simple linear interpolation between the rates of the two pure metals (Ghosh et al., 2004).

Bimetallic nanoparticles are particularly useful due to their additional degrees of freedom, composition and structure that may be adjusted in order to improve the catalytic behavior (Wilcoxon, 2009; Toshima and Yonezawa, 1998). Experimentally, PNP has a strong absorption at 400nm, (Panigarhi et al., 2007) which allows for an easy and reliable means to measure reaction rates by UV-Vis spectroscopy (Lee et al., 2008). The overall reaction rate is pseudo-first-order when both the metal catalyst and $NaBH_4$ are in excess. The reduction of PNP is, thus, an ideal model system for demonstrating the tunability of bimetallic nanoparticles in order to produce an optimal catalyst. In this mechanism, both molecules adsorb onto a surface before undergoing the bimolecular reaction. When $NaBH_4$ is in excess, the rate is controlled by the adsorption of PNP. The use of nanoparticles suspension as catalysts is not desirable due to their non-recyclability, which directs the conversion to solid state. The present chapter demonstrates the finding on these lines justifying the role of 3-APTMS. In chapter IV 3-APTMS mediated synthesis of AuNPs was observed in the presence of variety of

other reducing agents and the impact of reducing agents on the physical properties like dispersibility in solvents, pH tolerance and salt tolerance was discussed. Further, the role of 3-APTMS has also been demonstrated in simultaneous and sequential synthesis of bimetallic nanoparticles like PdAu using cyclohexanone and THF-HPO as reducing agents (Pandey et al., 2014; Pandey and Singh 2015b). The bimetallic NPs outclass the monometallic components in terms of properties like mimetic behavior and electrocatalytic behavior. The micellar activity of 3-APTMS allows control over the functional ability and dispersibility of as-generated trimetallic nanoparticles perfectly suitable for the reduction of PNP in homogenous medium. In addition to that, 3-APTMS is also prone to hydrolysis, condensation and polycondensation under suitable conditions and may be easily converted into a solid matrix retaining the catalytic activity of the nanomaterial. Different organic reducing agents along with 3-APTMS show selectivity towards the synthesis of noble metal nanoparticles. THF-HPO when used as a reducing agent with 3-APTMS can result in AuNPs (Chapetr III) and PdNPs (Pandey et al., 2014) but not AgNPs. Cyclohexanone, on the other hand, as a reducing agent can efficiently synthesize AuNPs, AgNPs and PdNPs but require different solvents as synthesis medium at different 3-APTMS concentrations making it difficult to carry out subsequent or simultaneous reductions for the synthesis of bimetallic or trimetallic nanoparticles. Similarly, formaldehyde, acetaldehyde, acetone and t-DMK can form AuNPs and AgNPs in the presence of 3-APTMS; however, out of these reducing agents, only formaldehyde enables the synthesis of PdNPs. For the synthesis of trimetallic nanoparticles, single protocol that can reduce all the three metal ions while complementing each other would be a better choice. The choice of formaldehyde seems quite reasonable for such conversion and fortunately interesting findings on the synthesis of trimetallic nanoparticles have been recorded. The present chapter reports

the synthesis of Pd, (AuPd) and Ag@(AuPd) nanoparticles using 3-APTMS and formaldehyde. The efficient reducing ability of 3-APTMS and formaldehyde enabled the controlled conversion of palladium cations into PdNPs within seconds. Trimetallic nanoparticles were synthesized via a bimetallic route, in which AgNPs are grown over preformed and simultaneously reduced bimetallic (AuPd) NPs. The selection of simultaneous (AuPd)NPs over sequential (Au@Pd)NPs will be discussed in detail later. The concentrations of 3-APTMS, formaldehyde and salts exploited during the synthesis of monometallic palladium, bimetallic PdAu and trimetallic Pd/Au/Ag nanoparticles are given in Table 6.1. Typically, 3-APTMS is added to the salt solution followed by formaldehyde addition; within 30 s, the colorless solution turned black in color. For the fabrication of trimetallic nanoparticles from (AuPd)NPs, Ag^{+} solution was added to the as-synthesized bimetallic nanoparticles.

Table 6. 1. Concentration of different constituents utilized during the synthesis of PdNPs, (AuPd)NPs and Ag@(PdAu)NPs.

NPs	Au^{3+}	Pd^{2+}	Ag^{+}	3-APTMS	HCHO
Pd	**-**	**10.7mM**	**-**	**0.5M**	**1.9M**
(AuPd)	**3.5mM**	**5.35mM**	**-**	**0.5M**	**1.9M**
Ag@(AuPd)	**2.3mM**	**3.6mM**	**2.4mM**	**0.5M**	**1.9M**

6.2. EXPERIMENTAL

6.2.1. Materials and Instrumentation

All reagents were used as-received. Palladium chloride, formaldehyde and silver nitrate purchased from Merck, India; tetrachloroauric acid hydrate purchased from HiMedia; 3-Aminopropyltrimethoxysilane was obtained from Aldrich Chem. Co. All other chemicals employed were of analytical grade. Aqueous solutions were prepared by

using doubly distilled-deionized water (Elga water purification system). The absorption spectra of the nanoparticles were recorded using a Hitachi U-2900 spectrophotometer. Transmission electron microscopy (TEM) images were recorded using a Morgagni 268D (Fei Electron Optics) operating at 200 kV. X-ray photoelectron spectroscopy studies were performed with an instrument from Kratos Analytical, a Shimadzu Group company, (Amicus XPS, UK).

6.2.2. Synthesis of PdNPs, (PdAu)NPs and Ag@(AuPd)NPs

In a typical process, 3-APTMS was added to a yellow-colored methanolic solution of $PdCl_2$ followed by stirring over a cyclomixer resulting in a colorless solution. The addition of formaldehyde to this solution resulted in a black-colored suspension of PdNPs in less than 30s. Similarly, for (AuPd) bimetallic nanoparticles, salts of Pd^{2+} and Au^{3+} were simultaneously reduced and stabilized using 3-APTMS and formaldehyde. Finally, for the synthesis of Ag@(AuPd) trimetallic nanoparticles, Ag^{+} was sequentially added to simultaneously synthesized (AuPd) bimetallic nanoparticles followed by stirring.

6.2.3. Conversion to heterogeneous catalyst.

The trimetallic Ag@(PdAu) thus synthesized was sonicated for 5 minutes followed by the addition of a small amount of dilute HCl (0.1M) and was allowed to stand for an hour. Addition of HCl initiates the condensation process resulting in the formation of nanoparticles encapsulated in a solid matrix. To remove any excess starting material, the nanoparticles were washed and sonicated 2–3 times with methanol.

6.2.4. p-Nitrophenol reduction and kinetic rate constant calculation

For the kinetic measurements, 30µl of 20mM PNP was added to 5 ml of water. To this was then added excess $NaBH_4$, so that its effective concentration in water is 0.05 M. Within seconds of $NaBH_4$ addition, 2 ml of it was taken in a cuvette. Decay of PNP at 400 nm was recorded after addition of the catalyst. The catalyst was diluted with methanol prior to addition. The data were analyzed according to the first order rate law. The absorbance at 400 nm was used to determine the concentration of PNP. The natural log of the absorbance at 400 nm was plotted against time, and the steepest part of the curve was fitted with a line, the negative slope of which was considered as the apparent rate constant, k_{app}. The rate constant was considered apparent because previous work by other groups has shown that the observed rate constant depends on the concentration of $NaBH_4$ as well as the starting concentration of PNP.

6.3. RESULTS

6.3.1. 3-APTMS and formaldehyde mediated Synthesis of mono, bi and trimetallic NPs

Since the rapid synthesis of trimetallic nanoparticles involve the active role of 3-APTMS and formaldehyde, it is important to review the contribution of amine containing trimethoxysilane group during the synthesis. Zhu et al. (2005) reported the synthesis of AuNPs based on the active participation of 3-(trimethoxysilylpropyl)diethylenemine, (TMSPdien). Time required for AuNPs formation from such triene alkoxysilane varied from 2 h to 23 h depending on the ratio of TMSPdien / Au^{3+}. The unique structure of TMSPdiene-Au complex has shown key point to the rapid autoreduction. When TMSPdien was replaced, by 3-APTMS they observed very slow conversion to nanoparticles and the prolonged reduction enabled the hydrolysis, condensation and polycondensation of silanol residue. These finding

revealed the reducing and stabilizing ability of 3-APTMS and also predict the essential requirement of additional reducing agent for real time and controlled nanoparticle synthesis. 3-APTMS alone will not form metal nanoparticles (AuNPs, AgNPs and PdNPs), it requires the participation of other mild reducing agents. Previous findings have evidenced the need of suitable organic reducing agent along with 3-APTMS for the conversion of Au, Ag and Pd to their respective nanoparticles.3-APTMS mediated synthesis of nanoparticles has been done by using several reducing agents like 3-GPTMS, THF-HPO, cyclohexanone, formaldehyde. 3-APTMS and formaldehyde assisted synthesis of AuNPs, AgNPs (previous chapters) and AuAg bimetallic nanoparticles (Pandey et al., 2015) have been documented. The present work deals with the 3-APTMS and formaldehyde mediated synthesis of Pd, (AuPd) and Ag@(AuPd) nanoparticles. A black-colored suspension of PdNPs is formed within seconds upon the addition of formaldehyde to a 3-APTMS capped Pd^{2+}solution. The UV-Vis spectra revealing the conversion of Pd^{2+} to PdNPs is shown in Fig. 6.1. The trimetallic NPs are synthesized via bimetallic Pd/Au nanoparticles, and the bimetallic NPs used for the synthesis of trimetallic nanoparticles can be fabricated by two routes. The first route is sequential, where constituent metal ions are reduced sequentially using 3-APTMS and formaldehyde i.e. AuNPs over PdNPs i.e. (Au@Pd). The second one is a simultaneous route where both $Au^{3+}$and Pd^{2+} salts are simultaneously reduced in the presence of 3-APTMS and formaldehyde i.e. (AuPd). The formation of bimetallic nanoparticles under both conditions has been evidenced spectrophotometrically as shown in the Fig. 6.2 (A & B). The concentrations of Pd^{2+}, Au^{3+}, Ag^{+}, 3-APTMS and formaldehyde used during the synthesis of the nanoparticles are provided in Table 6.1. Fig. 6.3 gives the TEM images of sequentially (Au@Pd) and simultaneously (AuPd) synthesized bimetallic nanoparticles with corresponding diffraction pattern.

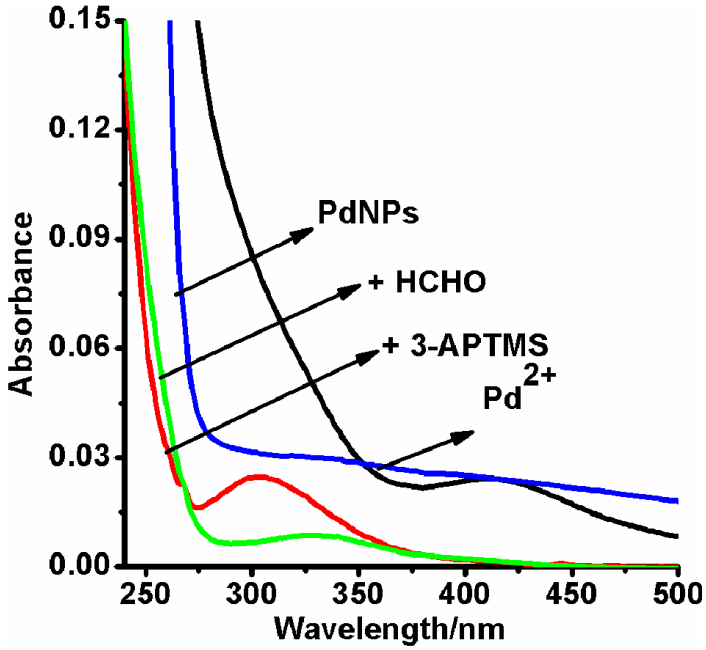

Figure 6.1. UV-Vis spectra of 10.7 mM $PdCl_2$ (i), 10.7 mM $PdCl_2$and 0.5M 3-APTMS (ii), 10.7 mM $PdCl_2$, 0.5 M 3-APTMS and 1.9 M formaldehyde (iii) and PdNPs formed (iv).

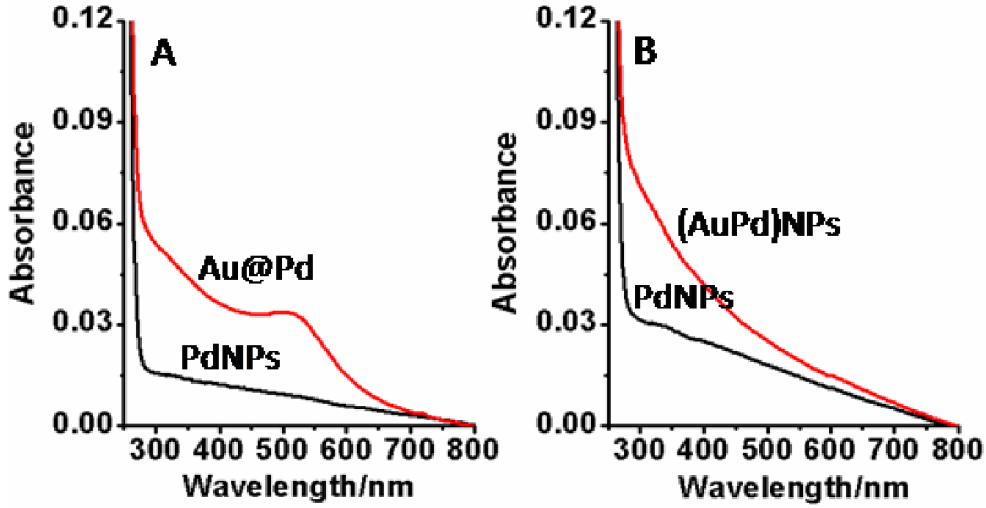

Figure 6.2. UV-Vis spectra of sequentially (A) and simultaneously (B) made AuPd bimetallic nanoparticles.

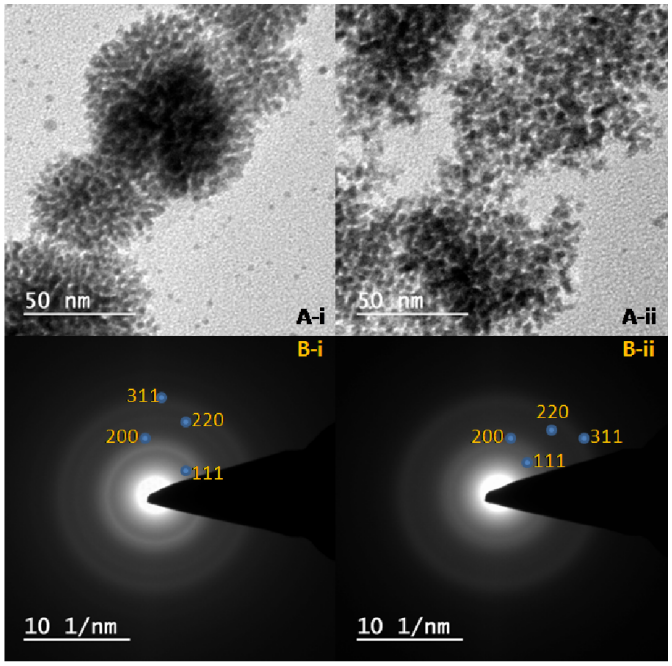

Figure 6.3. TEM images and diffraction pattern of Au@Pd (A-i, B-i) and AuPd (A-ii, B-ii).

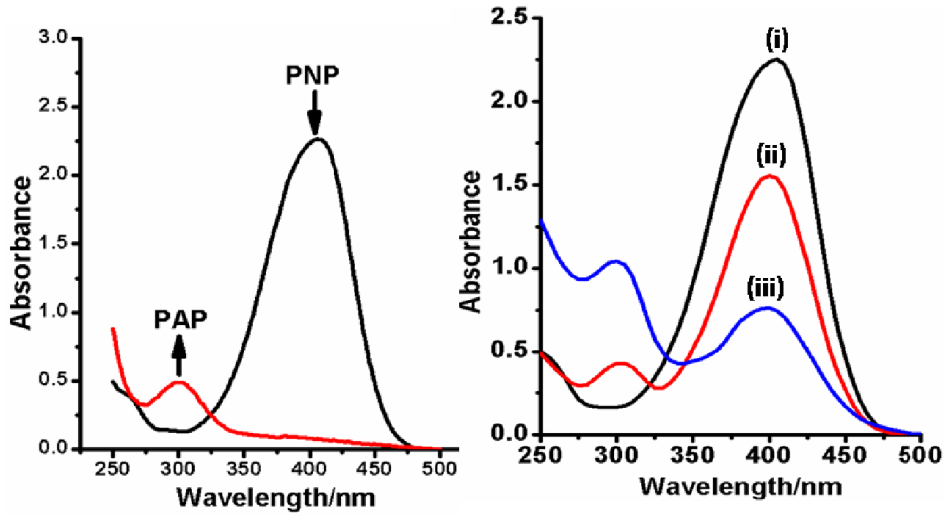

Figure 6.4. Typical UV-Vis spectra of PNP and PAP [left] and time dependent absorbance of PNP in the presence of excess $NaBH_4$ without catalyst (i); with (Au@Pd) (ii)and (AuPd) (iii) [right].

The electron diffraction patterns of PdAu and Au@Pd exhibited four rings assigned to (111), (200), (220) and (311) lattice planes. To select the best bimetallic moiety for the

trimetallic nanoparticle synthesis, the catalyzing ability of both simultaneously and sequentially made (Au/Pd) bimetallic nanoparticles for the reduction of PNP was monitored and compared. Simultaneously made (AuPd)NPs were more catalytic compared to sequentially made (Au@Pd)NPs towards PNP reduction to PAP as shown in Fig. 6.4, where all the conditions were same except that the catalysts were made following different protocols (concentration of metal constituent of the catalyst, 3-APTMS and formaldehyde was also kept the same).

6.3.2. Structural characterization

Fig. 6.5 shows the spectral recording for monometallic Pd, bimetallic (AuPd) and trimetallic Ag@(AuPd) nanoparticles. The peak corresponding to AuNPs SPR in bimetallic (AuPd) is not visible in this figure but as the concentration of Au^{3+} is increased for fabricating (AuPd) bimetallic nanoparticles, the peak corresponding to AuNPs becomes more and more visible as given in the Fig.6.6A. Fig. 6.6B gives the spectral recording for the addition of a fixed Ag^{+} concentration to (AuPd) nanoparticles fabricated at different Au^{3+} concentrations. The TEM images of the Pd, (AuPd) and Ag@(AuPd) nanoparticles with corresponding diffraction patterns are given in Fig. 6.7-Fig.6.9. PdNPs show aggregates of very small structures leading to clusters (nearly 2–4 nm) displaying a flower-like arrangement (Fig. 6.7). Aggregate formation is due to the self-assembling nature of 3-APTMS. The self-assembling nature also confirms the capping ability of 3-APTMS on the palladium surface. The TEM image of (AuPd) bimetallic nanoparticles (Fig. 6.8) also displays aggregates of small units but they are more dispersed and less aggregated than PdNPs making a much larger surface area available for any catalytic reactions. The TEM image of Ag@(AuPd) trimetallic nanoparticles (Fig.6.9) clearly shows discrete pear-shaped AgNPs attached to (AuPd) bimetallic nanoparticles, further enhancing the surface area.

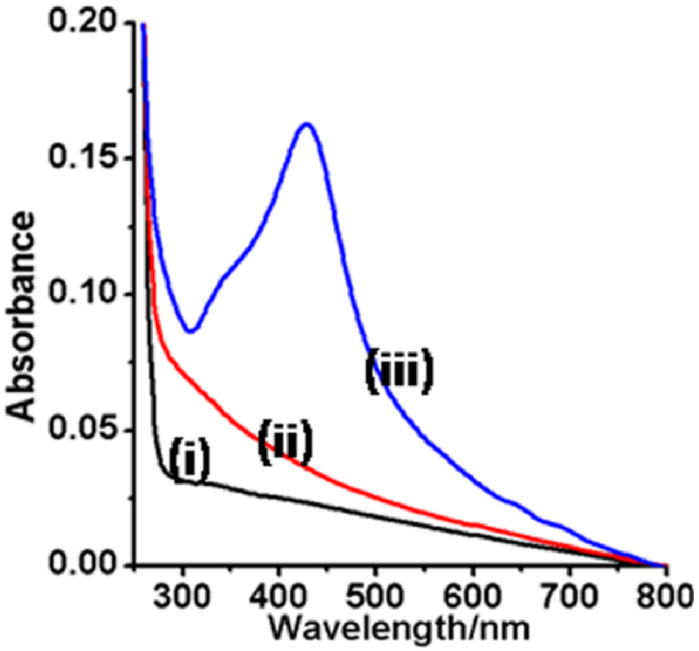

Figure 6.5 UV-Vis spectra of PdNPs, (AuPd)NPs and Ag@(AuPd)NPs

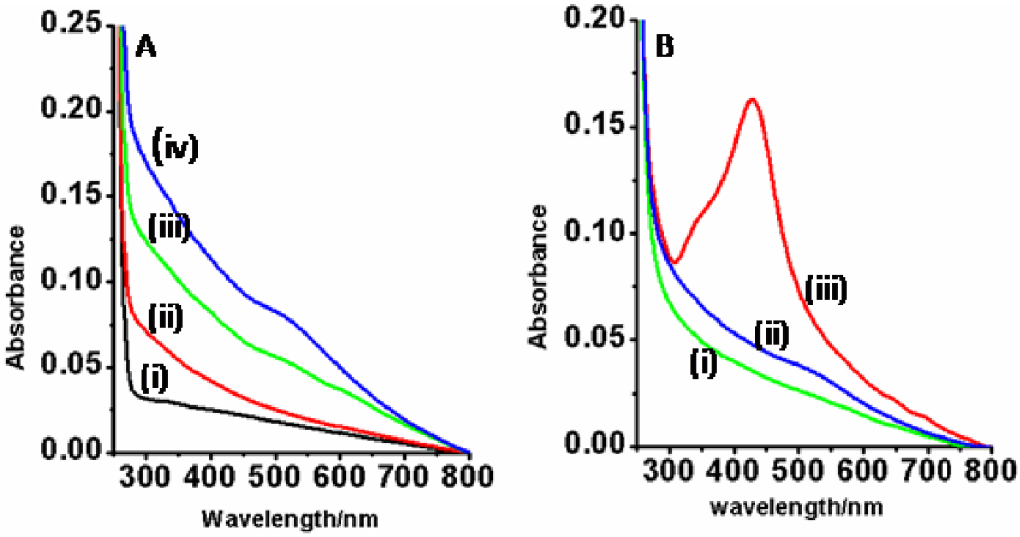

Figure6.6. UV-Vis spectra of (A) Bimetallic (PdAu) NPs made at increasing concentration of Au^{3+} and (B) Trimetallic Ag@(PdAu) NPs made by adding constant concentration of Ag^{+} to (PdAu) made using different Au^{3+} concentration.

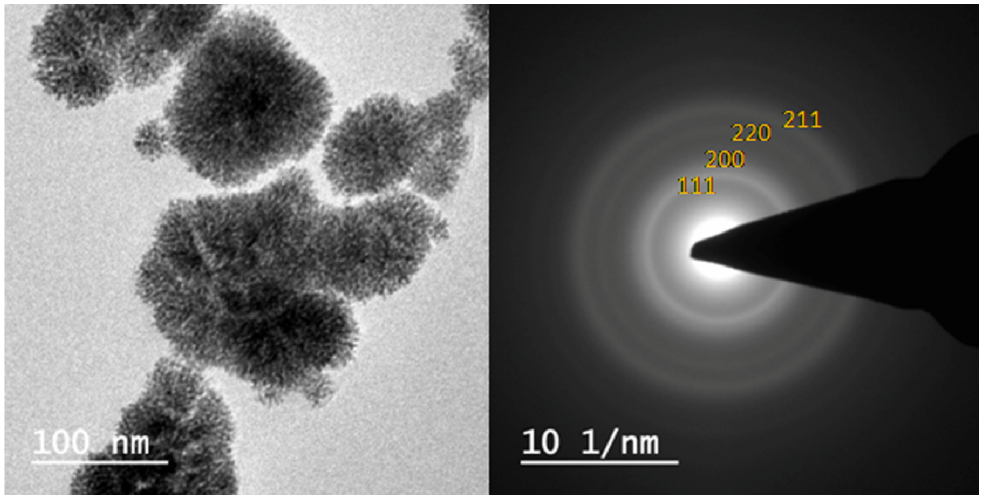

Figure 6.7. TEM image (left) and diffraction pattern (right) of PdNPs.

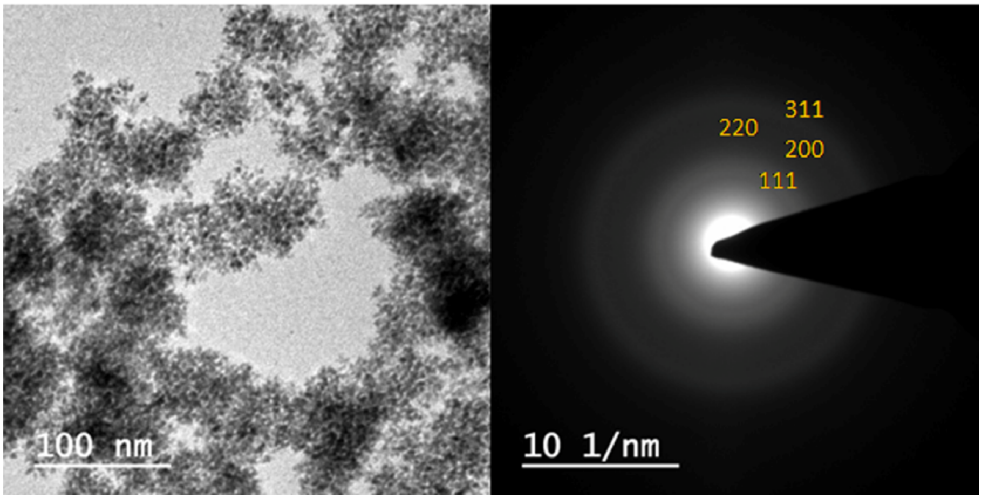

Figure 6.8**.** TEM image (left) and diffraction pattern (right) of (PdAu)NPs.

The chemical composition and the chemical state of constituent metals in the mono-, bi- and trimetallic nanoparticles were analyzed by XPS as shown in the Fig. 6.10 - Fig. 6.12.

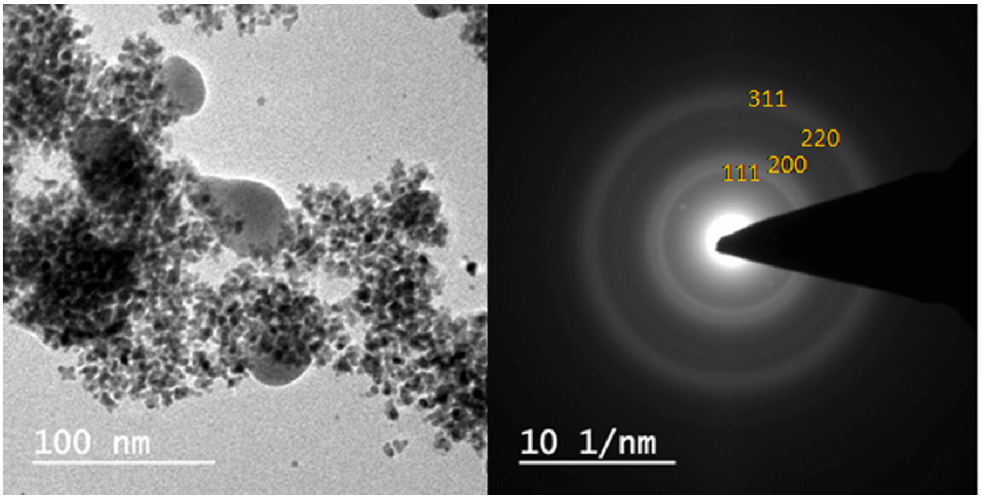

Figure 6.9. TEM image (left) and diffraction pattern (right) of Ag@(AuPd)NPs.

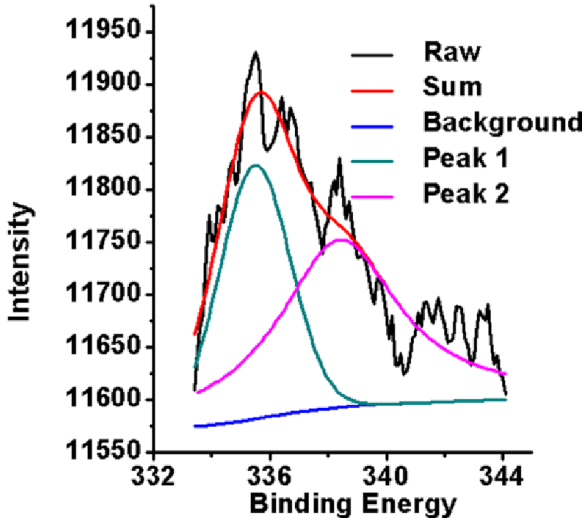

Figure 6.10. XPS spectra of Pd in PdNPs.

6.3.3. Homogenous catalysis

PNP reduction to PAP was tested as a model reaction for comparing the catalytic performances of monometallic PdNPs, bimetallic (AuPd)NPs and trimetallic Ag@(AuPd)NPs, with an excess amount of $NaBH_4$. As shown in Fig.6.13A, the

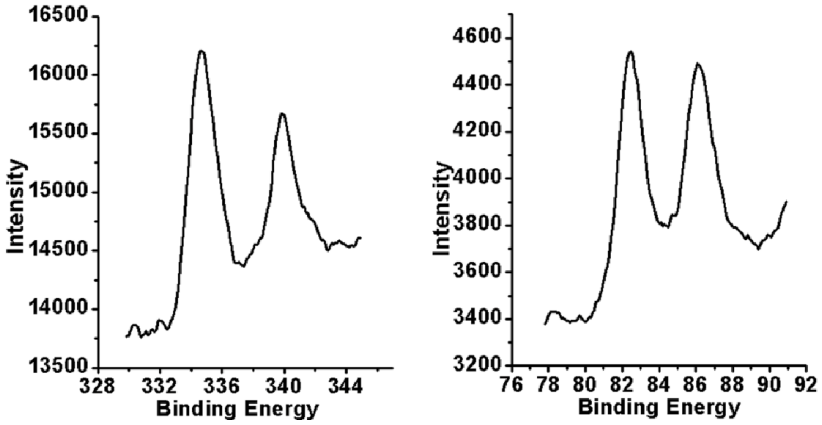

Figure 6.11. XPS spectra of Pd (left) and Au (right) in AuPd bimetallic NPs.

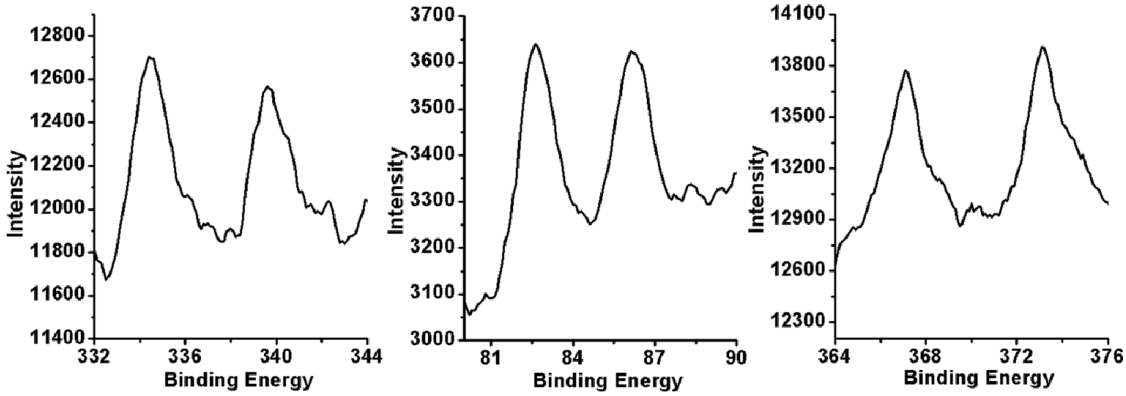

Figure 6.12. XPS spectra of Pd (left), Ag (middle) and Au (right) in Ag@AuPd trimetallic NPs.

---

reduction of PNP to PAP is evidenced by a decrease in absorbance at 400 nm and a new absorbance peak appearing at 315 nm associated with the formation of PAP. The yellow colored solution changes to colorless solution on the formation of PAP. The reaction completed in seconds with trimetallic Ag@(AuPd) nanoparticles taking the least time, monometallic PdNPs taking the most and simultaneously made bimetallic (AuPd)NPs being in between the two.

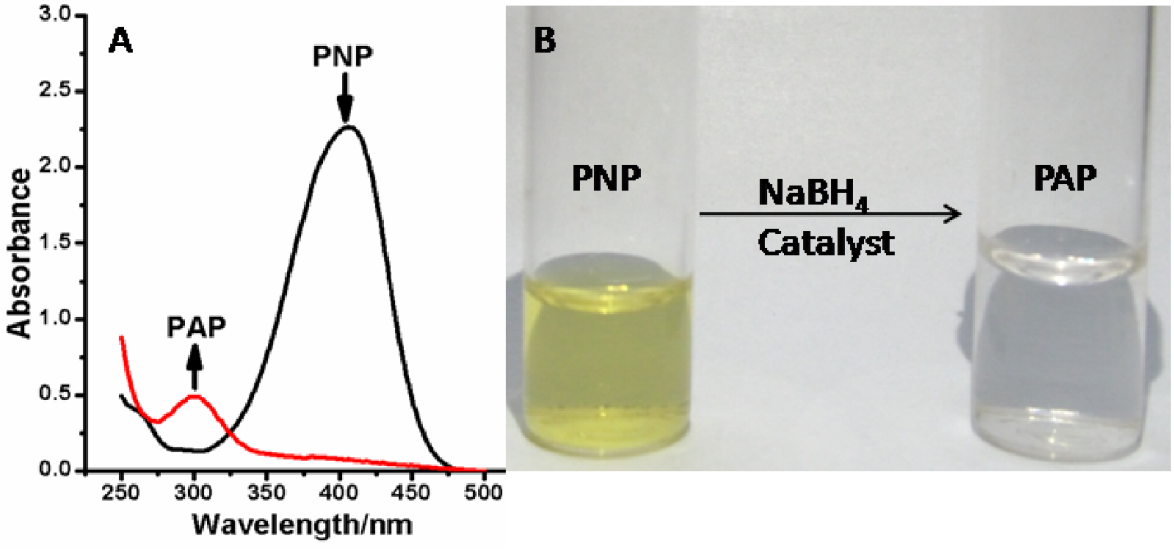

Figure 6.13. Typical UV-Vis spectra for reduction of PNP to PAP (left). Pictorial representation for showing transition from yellow color of PNP to colorless PAP.

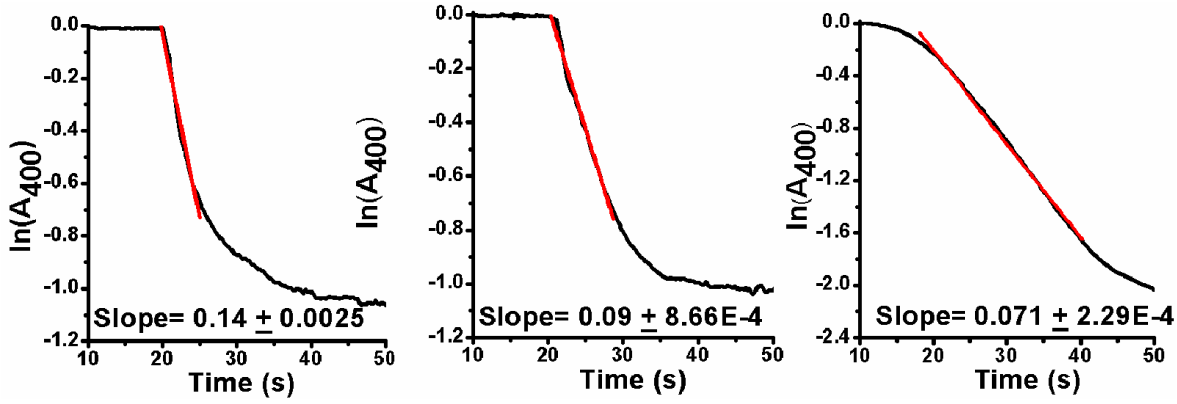

Figure6.14. Plot of ln(A_{400}) versus time for the reduction of 4-NP for Ag@(AuPd)NPs (left), (AuPd)NPs (middle) and PdNPs (right).

Fig. 6.14 shows the decrease in absorbance of PNP (400nm) with time for three different catalytic system [PdNPs (left), AuPdNPs (middle) and Ag@(AuPd)] and the arrows in Fig. 6.14 show the point where nanoparticles were added to the PNP solution. Because the reaction is pseudo first-order in the presence of excess $NaBH_4$, the slope of

a plot of the natural log of the absorbance at 400 nm yields the apparent reaction rate,k_{app}. Rate constants were calculated by plotting a graph between lnA_{400nm} and time.

6.3.4. Heterogeneous catalysis

Heterogeneous systems are preferred over homogenous systems for their economic importance. They can be used again and again for catalyzing reactions of interest, thereby evading the loss that homogeneous systems incur. Besides stabilizing the nanoparticles, 3-APTMS also plays an important role in converting a homogeneous nanoparticle suspension into a solid matrix with the support of a $–Si(OMe)_3$ group at one end of 3-APTMS. In an attempt to convert the homogenous catalyst to a more economic heterogeneous catalyst, a colloidal suspension of the most catalytic trimetallic Ag@(PdAu) was selected. To the presynthesized trimetallic nanoparticle was added a small amount of HCl (0.1M) and the resulting solution was kept at 50–60°C. HCl initiated the Si–O–Si linkages between 3-APTMS molecules. Within an hour, nanoparticles embedded in a solid matrix were obtained as shown in Fig.6.15. The heterogeneous catalyst thus formed was found to be catalytic in nature against PNP reduction as shown in Fig.6.16 with added advantages of regeneration and recyclability. Fig. 6.15 shows the conversion of the sol to the solid matrix upon addition of HCl. The solid obtained was sonicated in methanol using an ultrasonicator to get rid of any unwanted material. Usually, for the conversion of a homogenous system to a heterogeneous system, the nanomaterial surface needs modification such that the size is the least affected, and also some support like TiO_2, ZnO, etc. over which the material is to be adsorbed is required. The use of 3-APTMS is perfectly suited for both tasks and thus with it being the stabilizer without any further modification, the homogeneous suspension is converted to a heterogeneous system simply through the addition of HCl.

The stability of AuNPs and AgNPs to HCl is proved in Fig.6.17 and stability for PdNPs is dealt later in discussion part.

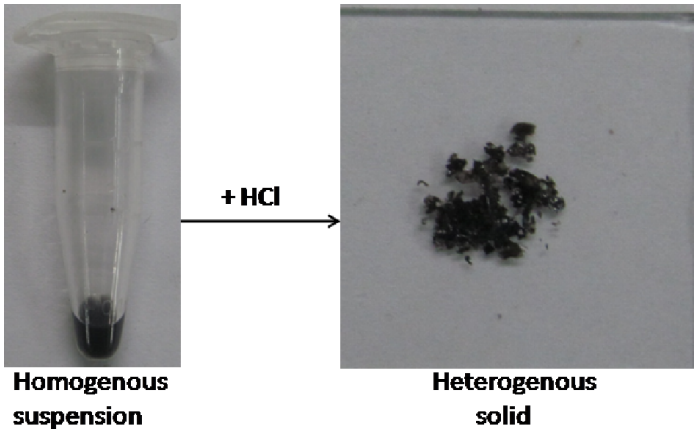

Figure 6.15. Pictorial representation for the conversion of Homogenous suspension of 3-APTMS and formaldehyde mediated trimetallic NPs to heterogenous solid matrix in the presence of HCl.

6.4. DISCUSSION

6.4.1. Structural analysis

The disappearance of the peak at 415 nm for Pd^{2+} (Fig. 6.1) together with the appearance of black color, and with the evidences from other characterization studies discussed above the synthesis of PdNPs from Pd^{2+} in the presence of 3-APTMS and formaldehyde is confirmed. The UV-Vis spectra of sequentially and simultaneously made bimetallic nanoparticles shown in Fig. 6.2 reveal that (Au@Pd) gave peak at around 520nm in spectral recording, corresponding to AuNPs, whereas spectrum of simultaneously made (AuPd)NPs was devoid of any peak around 520nm.

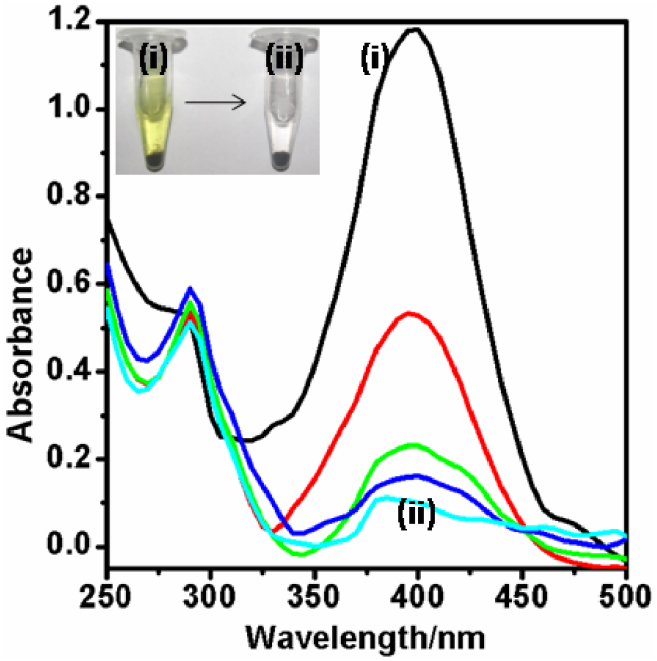

Figure 6.16. UV-Vis spectra displaying the decrease in absorbance value for the peak at 400nm corresponding to PNP in the presence of powder catalyst and excess $NaBH_4$. Inset shows the image for the same.

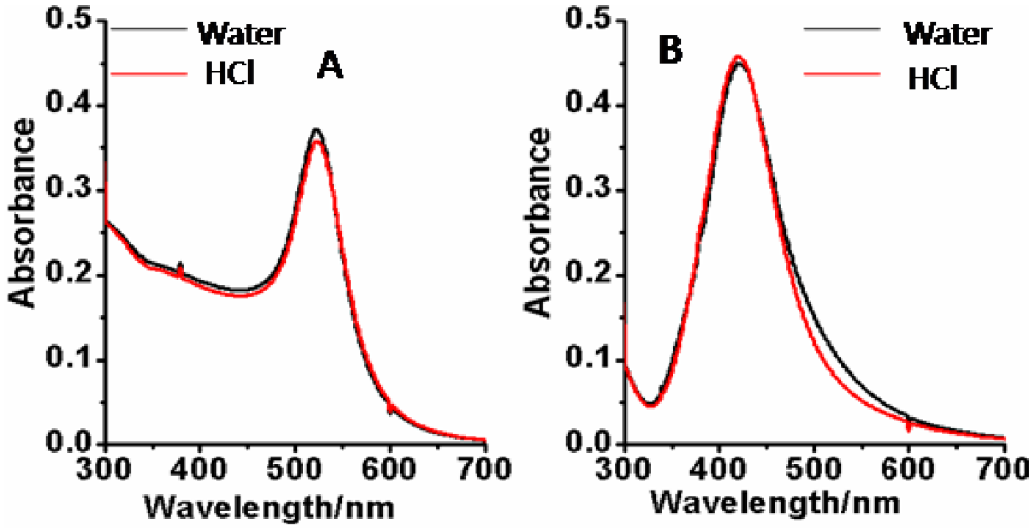

Figure 6.17. UV-Vis spectra of showing the stability of AuNPs (A) and AgNPs (B) in the presence of HCl relative to water.

Thus, it gave an idea about the structural difference of two types of bimetallics which is corroborated by the TEM images and diffraction pattern of both types of bimetallics

given in Fig. 6.3.The d-spacing values for the ring indexed to (220) corresponded to Au while the others matched with PdNPs (Table 6.2).

Table 6.2 d-spacing values for rings obtained in diffraction pattern of synthesized nanoparticles

NPs	d1 (111)	d2(200)	d3(220)	d4(311)
Pd	**2.2805**	**1.9735**	**1.3592 (Pd)**	**1.15306 (Pd)**
(AuPd)	**2.2805**	**2.05245 (Au)**		**1.1795 (Pd)**
Ag@(AuPd)	**2.2805**	**2.0322(Au Ag)**	**1.3592 (Pd)**	**1.1661 (Pd)**
Au@Pd	**2.2805**	**2.05245(Au)**	**1.3592 (Pd)**	**1.15306 (Pd)**

The presence of rings corresponding to both Au and Pd rules out the possibility of alloying in both cases. PdAu bimetallic nanoparticles, when made simultaneously, take a core–shell structure. Due to difference in atomic weight of Pd (106.42) and Au (196), there is a contrast difference in their images as shown in Fig. 6.3. Also, during simultaneous synthesis, the appearance of a reddish sol is followed by blackening of the same, thus proving that gold nanoparticles are formed before PdNPs and hence the core–shell structure. In the case of sequential synthesis, Au@PdNPs aggregates remain as such without any segregation of PdNPs, upon addition of AuNPs, displaying uniform gradation as in PdNPs. Besides, AuNPs can also be seen scattered in spherical shapes in the TEM images of (Au@Pd)NPs, far separated from the clusters of PdNPs. Thus, it is concluded that simultaneously made (AuPd)NPs take a core–shell structure while Au@Pd NPs take no specific design.

6.4.2. Bimetallic: (AuPd) vs (Au@Pd)

To select the bimetallic (Au@Pd or AuPd) for trimetallic (Ag@AuPd) synthesis PNP reduction reaction was chosen as a parameter. The bimetallics were made using same concentration of constituent ions and differed only in the protocol for their synthesis. The reaction conditions were kept same except the catalyst type and the absorbance value for PNP was recorded at a fixed time for both systems. The results as shown in Figure 6.4 indicate that (AuPd)NPs are more catalytic than (Au@Pd)NPs. The difference in the catalytic behavior of the two can be easily explained by viewing the TEM images shown in Fig. 6.3A and B. From the TEM images, it can be inferred that the sequential addition of Au^{3+} over PdNPs has no effect on the PdNP aggregates, whereas, simultaneously made AuPdNPs are more dispersed and less aggregated, providing greater surface area for its catalytic role. Based on these results, simultaneously made (AuPd)NPs are chosen for the fabrication of the trimetallic Ag@(PdAu)nanoparticles. As the trimetallic nanoparticle synthesis involves two steps: first is the simultaneous synthesis of AuPd and second is the Ag^{+} addition over simultaneous synthesized AuPd, it is therefore referred to as a "**one-pot two-step synthesis**". The UV-Vis spectra for the mono, bi and trimetallic nanoparticles with corresponding peaks are given in Fig.6.5.

The AuPd bimetallic used for the synthesis of trimetallic was monitored spectrophotometrically under increasing concentration of Au^{3+} followed by the study on the effect of adding constant concentration of Ag^{+} to the bimetallic made using different concentration of Au^{3+}. Analysis of Fig.6.6 (A&B) proves that the SPR at 420 nm corresponding to AgNPs can only be seen when the Au^{3+} concentration is low i.e. 2 mM. In other cases where the Au^{3+} concentrations are 5 mM and 10 mM, no SPR corresponding to AgNPs is visible. From these observations, it is concluded that Ag and

Au with very close lattice constants undergo alloy formation but when Ag^{+} concentration is more than needed for the available gold content, it gives SPR corresponding to AgNPs (seen as pear-shaped attachment to already formed AuPd bimetallic nanoparticles).

6.4.3. Chemical characterization

XPS results (Fig. 6.10-Fig. 6.12) show that the binding energy of Pd 3d in AuPd and Ag@(AuPd) has shifted to a lower value compared to that in PdNPs as shown in Table 6.3. Similarly, the binding energy of Au 4f in Ag@(AuPd) has shifted to a higher value compared to that in AuPd. These shifts demonstrate that some electrons are transferred from Au to Pd in both bimetallic and trimetallic nanoparticles. These spectra confirm the presence of one metal (Pd), two metals (Pd, Au) and three metals (Pd, Au, Ag) in the monometallic, bimetallic and trimetallic nanoparticles, respectively. The binding energy data reveal that Pd, Au and Ag have been reduced to their atomic states in bimetallic (AuPd) and trimetallic Ag@(AuPd) NPs.

Table 6.3 Binding Energy data for individual components of PdNPs, (AuPd)NPs and Ag@(AuPd).

Nanoparticles	**Pd (Binding Energy)**	**Au(Binding Energy)**	**Ag(Binding Energy)**
PdNPs	**335.5eV**	**-**	**-**
AuPdNPs	**334.6eV**	**82.5eV**	**-**
Ag@AuPdNPs	**334.39eV**	**82.6eV**	**367.1eV**

However, the XPS spectra of PdNPs indicate partial conversion to PdNPs. Analysis of XPS data for PdNPs indicate the presence of Pd^{2+} with Pd^{0}. Meanwhile, Pd^{2+}

conversion to Pd^0 is complete in (AuPd)NPs which means that Au^{3+} facilitates the conversion of Pd^{2+} to PdNPs.

6.4.4. Synergistic effect

It is to be noted that monometallic AuNPs and AgNPs, if fabricated by exploiting the same concentration of 3-APTMS as in trimetallic nanoparticles, do form but are relatively less stable compared to the trimetallic NPs with all the three (Pd, Au and Ag) constituents. Also, PdNPs alone are less catalytic with aggregated structures but induction of AuNPs and AgNPs makes them more catalytic with greater surface area. Such an effect can be easily explained by the synergism of the parent components in the bimetallic and trimetallic nanoparticles. In addition to that, the presence of AuNPs and AgNPs also facilitates the complete reduction of Pd^{2+} to Pd^0. The synergism in multimetallic nanoparticles also explain the relatively increased stability of trimetallic nanoparticles compared to monometallic ones made using the same 3-APTMS concentration.

6.4.5. Catalysis

In the presence of excess $NaBH_4$ and sufficient catalyst, the reaction is pseudo-first-order and depends only upon the concentration of PNP in the solution. The light yellow-colored solution of PNP turns dark yellow upon the addition of $NaBH_4$ due to formation of nitrophenolate ions. With the addition of catalyst, the yellow color of the solution fades away with time (Fig. 6.13, right side). This progress of reaction can be monitored spectrophotometrically. PNP reduction in the presence of $NaBH_4$ is fast when performed in solution with coinage metal catalysts. PNP is a strong visible absorber with maximum absorbance at 400nm.The rate constant was found to increase gradually from monometallic PdNPs to trimetallic Ag@(AuPd)NPs. Both PNP and

$NaBH_4$ get adsorbed on the catalyst converting it to PAP. The concentrations of PNP and $NaBH_4$, the amount of catalyst and the rate constant value obtained thereafter are given in Table 6.4. From the results recorded in Table 6.4, it can be seen that trimetallic nanoparticles have the highest rate constant value which might be assigned to the increased surface area due to attachment of pear-shaped AgNPs. Besides, Pd is fully reduced both in (AuPd) and Ag@(AuPd) resulting in higher catalytic activity compared to that in PdNPs only. To gain deeper insight, the rate constants for AuNPs, AgNPs and (AuAg) nanoparticles was also calculated. The catalyzing ability was in the order of (AuAg)NPs >AuNPs>AgNPs. Thus, there are two reasons for the enhanced catalytic activity of Ag@(AuPd): physical attachment of the AgNPs at the surface of (PdAu) and alloying of AgNPs with AuNPs.

Table 6.4. A comparative study on the catalyzing ability of nanoparticles [Pd, (PdAu) and Ag@(PdAu)] during the reduction of PNP (0.015M) to PAP in the presence of excess $NaBH_4$ (0.05 M).

Catalyst	PNP (mM)	NaBH4(M)	Kapp (s-1)
PdNPs	**0.12**	**0.05**	**0.071 ± 0.0025**
AuNPs	**0.12**	**0.05**	**0.051 ± 2.40×10−4**
AgNPs	**0.12**	**0.05**	**0.028 ± 9.70×10−5**
AuAgNPs	**0.12**	**0.05**	**0.065 ± 6.12×10−4**
AuPdNPs	**0.12**	**0.05**	**0.090 ± 8.66×10−4**
Ag@(AuPd)NPs	**0.12**	**0.05**	**0.140 ± 2.29×10−4**

6.4.6. Conversion of colloidal suspension to solid matrix

In the very first chapter it was mentioned that one of the use of 3-APTMS is for the conversion of homogenous suspension to heterogeneous solid matrix. As shown in

Scheme 6.1, trimethoxy groups attached to silica can be hydrolyzed in the presence of HCl, converting them to hydroxyl groups that undergo condensation resulting in the formation of a Si–O–Si solid matrix. The additions of acid to NPs, in the present case do not disturb the SPR of the same as shown in Fig.6.17 (right side).

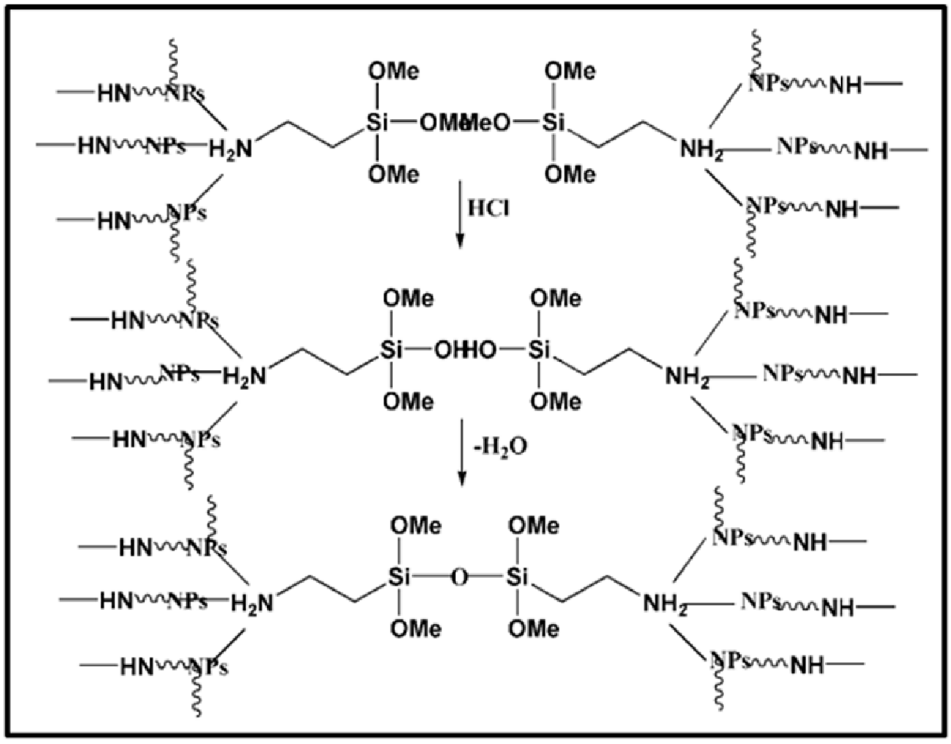

Scheme 6.1. Mechanism for the conversion of 3-APTMS homogenous suspension to heterogenous matrix on the addition of HCl.

There is no SPR corresponding to PdNPs. Thus, the effect of acids on PdNPs could not be monitored spectrophotometrically. However, indirectly by measuring the catalytic activity of PdNPs in the presence and absence of an acid, their stability against acids was confirmed. Thus, the nanoparticles (Pd, PdAu and Ag@(PdAu) do not get affected by the addition of HCl (0.1 M) during the conversion to solid heterogeneous matrices. So, the amine capped nanoparticles get embedded in a solid matrix created by Si–O–Si linkages without undergoing any agglomeration upon addition of HCl.

6.5. CONCLUSION

In summary, a simple and rapid method has been described for the synthesis of PdNPs, within seconds under ambient conditions, from 3-APTMS and formaldehyde. The synthesis is further extended to Ag@(AuPd) trimetallic nanoparticles via (AuPd) bimetallic nanoparticles. The as-synthesized monometallic, bimetallic and trimetallic nanoparticles are characterized by UV-Vis spectroscopy, TEM and XPS. The trimetallic nanoparticle suspension is found to be highly catalytic for PNP reduction to PAP with a rate constant value of $0.14 \pm 0.0025\ s^{-1}$. 3-APTMS used serves a dual purpose: (1) as a stabilizer and (2) as a precursor to the solid matrix. The point that further favours the conversion of the homogenous suspension to the solid matrix is that the nanoparticles do not get affected by HCl addition. Upon addition of a small amount of acid, Si–O–Si linkages are formed leading to the solid matrix being embedded with nanoparticles. This is used as a heterogeneous catalyst which can be recycled easily and can be used as a catalyst again.